EFINS-65-88

ABUNDANCES AND ENERGY SPECTRA FOR NUCLEI OF GALACTIC ORIGIN ABOVE 20 MEV PER NUCLEON

G. M. Comstock, C. Y. Fan and J. A. Simpson
Enrico Fermi Institute for Nuclear Studies
University of Chicago

Presented at International Conference on Cosmic Rays,
London, 6 - 17 September 1965

To be published in the
Proceedings of the International Conference on Cosmic Rays, London
by the Physical Society, London

Abundances and Energy Spectra for Nuclei of Galactic Origin Above 20 MeV per Nucleon

G. M. Comstock, C. Y. Fan and J. A. Simpson
Enrico Fermi Institute for Nuclear Studies
University of Chicago

14275

Abstract. The individual chemical abundances of nuclei with charge Z extending from Z = 2 to Z = 14 in the energy range 20 to 300 Mev/nucleon have been measured in interplanetary space on the OGO-I satellite for ~ 150 hours in October and November 1964. At higher Z, two charge groups were measured, including the Fe-group. The energy spectra for C, O and Ne are shown to be remarkably flat and different from the helium spectrum measured simultaneously over the same energy/nucleon range. It is concluded that these spectral differences exist in the cosmic radiation outside the solar system. The relative abundances for $6 \leq Z \leq 14$ display an even-odd Z ratio of approximately 8:1. Li, Be and B, and the Fe-group are present with about the same relative abundances as observed at higher energies. It is suggested that the rate of particle acceleration for a wide range of Z competes effectively with the rate of ionization loss at these low energies. The measurements were made with solid-state silicon detectors and anticoincidence scintillators arranged to measure energy-loss and total energy.

I. Introduction

From measurements in interplanetary space on the OGO-I satellite‡ we report preliminary results for the chemical abundances of nuclei with charge Z extending from Z = 2 to Z = 14 in the energy range 20 to 300 Mev/nucleon. For higher Z, our measurements are limited to two charge groups, one being the Fe-group. This nuclear charge and energy range is of fundamental interest for investigating the origins of the cosmic radiations insofar as various hypotheses predict different relative chemical abundances and energy spectra for these nuclei as they undergo acceleration, and as they propagate through the interstellar medium.

The results are based upon more than 150 hours of data over the period October - November 1964. This was near the time of minimum solar modulation of the galactic flux as determined by the presence of galactic helium nuclei down to 7 Mev/nucleon (Fan, Gloeckler and Simpson 1965). A finite flux of medium and heavy Z-groups of nuclei above ~ 50 Mev/nucleon were observed by Fichtel, Guss and Neelakantan (1965) in 1963. Hence other nuclei with the same velocity and magnetic rigidity should have access to the orbit of Earth at this time.

II. Instrumentation and Data Analysis

Figure 1A is a cross section view of the particle telescope detector elements. D_1 and D_2 are two gold-silicon surface barrier detectors of 4.5 cm^2 sensitive area and silicon thickness 550μ. The depletion depths

are 200μ. A charged particle must penetrate both D_1 and D_2 to initiate a measurement of energy loss (dE/dx) in D_1. Particles which also penetrate to the CsI scintillator D_3 but not to the scintillators D_4, or D_5, also initiate the measurement of total energy deposited in D_3 as illustrated by particle trajectory a in Figure 1A. Particles which penetrate D_1 and D_2, but not D_3 are in the general energy range ~ 10 to 30 Mev/nucleon. Particles which penetrate to D_4 as shown by trajectory b in Figure 1A (>300 Mev/nucleon) are not investigated in this paper.

The response of the detector and the coincidence logic will be published later, but they are generally similar in principle to the IMP-I telescope (Fan, Gloeckler and Simpson 1965). The pulse height analyzers associated with detectors D_1 and D_3 each independently have two dynamic ranges of operation.

Raw data are plotted in Fig. 1 for the low gain modes of the D_1 and D_3 analyzers. The numbers representing the data points show how many analyzed events were found within the same D_1 and D_3 channel numbers. The calculated solid line curves take account of the window mass (0.039 g/cm^2), detector absorbers, the mean angle of incidence and are corrected for inflight calibrations. Since isotopes of an element are not resolved, the isotope used to calculate each curve is the one most likely to be found in nature. In the discussion which follows we shall call these curves the tracks for the distribution of data points for the nucleus being analyzed.

The technique used to analyze helium in the IMP-I experiment (Fan, Gloeckler, Simpson 1965) was used for these data. The difference between the D_1 channel number for a given solid curve shown in Figure 1 is called the D_1 channel deviation. Figure 2 shows the distribution of observed D_1 channel deviations. Each distribution contains the number of events occurring in the D_3 channel given in the caption. The distributions indicate the true detector resolution only for the element whose track is used as the center for the measurement; i.e. centered on "0" deviation. The abundances for N, F, Na and Al are upper limits.

The error bars are the standard deviations which are the largest sources of error for the data in Figures 3 and 4. The relative abundances are normalized to Oxygen which we find has an absolute flux of 5.4×10^{-3} nuclei/m^2-Sec-Sr-Mev/nucleon.

Boron is also present in the data of Figure 1, and extends into another mode where, in addition, Helium, Lithium and Beryllium are analyzed. The results for Li, Be, and B in our analysis is limited to $> \sim 60$ Mev/nucleon at present in order to avoid background corrections.

Resolution of individual elements breaks down at high Z, but due to the onset of nonlinearities in the instrument for larger pulses, heavier nuclei in the range 150 to 250 Mev/nucleon are readily measured. Abundances for the Fe-group (VH nuclei) and the heavy group ($15 \leq Z \leq 25$) are shown in Figure 3.

III. Abundances of Nuclei

Although there is an over-all similarity between the relative abundances for $Z \geq 6$ in Figure 3 and the "cosmic" abundances reported in the literature, there are some striking differences. For example, the relative abundance of N is low, and the very heavy elements are greatly enriched.

The even-odd Z ratio for the abundances, especially for $6 \leq Z \leq 10$ nuclei, is ~ 8:1 in the 20 to 300 Mev/nucleon range. This is at least as large, or possibly larger, than observed at high energies. This result tends to exclude spallation in interstellar space, or in the source, as the dominant process shaping the composition and energy spectra of medium Z nuclei at low energies. Even with the build-up of radioactive decay products from spallation the even-odd Z effect does not exceed 3:1 (Peters 1962; Badhwar, et al. 1962). Also, our high abundance of the Fe-group suggests that the Fe-group flux does not disappear due to spallation, or to ionization loss. Finally, if we assume that the abundance of the nuclear group $15 \leq Z \leq 25$ is dominated by the abundances of the even Z particles, then the average abundance of an even Z nucleus in this interval is similar to N, F, or Na. These abundances are much lower than would be expected from a charge distribution of nuclei originating in Fe-group spallation. The only argument we find in favor of spallation as an important process is the relatively high abundance of Li, Be and B. In view of the over-all results it may be worth re-examining the possible origin of these light elements.

The following table compares the relative abundances in Z-groups commonly used in the literature:

	L/He	M/He	L/M	H/M	VH/H
OGO-I	0.019 ± 0.004	0.064 ± 0.006	0.30 ± 0.05	0.38 ±0.06	0.42 ±0.09
Waddington (1963) (>1.5 $\frac{\text{BeV}}{\text{nuc}}$)	0.018	0.065	0.35	0.34	0.35-0.38

L = $3 \leq Z \leq 5$; M = $6 \leq Z \leq 9$; H = $10 \leq Z \leq 25$; VH = $26 \leq Z$.

IV. Energy Spectra for C, O and Ne

The flat spectra for C, O and Ne are the most remarkable feature in Figure 4. We recognize that some nuclei at the upper energy ranges in Figure 4 will undergo fragmentation in the CsI crystal producing fragments with ranges extending into the D_4 detector so that they are excluded in our preliminary analysis. Figure 4 does not yet include this correction, but it has an upper limit of <25 percent for the highest energy point, which will not bring the spectra into agreement with the observed helium spectrum of $E^{+1.3}$ in this energy range at this time. Our spectra are flatter than the medium Z group spectrum given by Fichtel, Guss and Neelakantan (1965), but we believe this is accounted for by the change in modulation which occurred between 1963 and 1964. Since the relative abundances of all particles with mass-to-charge ratio two are likely to be independent of solar modulation, we conclude that the observed differences in the spectrum of helium and the higher Z nuclei in Figure 4 are characteristic of spectral differences outside

the solar system, i.e. in nearby interstellar space. The possibility of a small solar component of C, O and Ne at the lowest energies cannot be excluded on the basis of these data, but we have searched for, and not found so far, a contribution of this kind. This flattening of the spectra may arise from the Z^2 dependence on the rate of ionization loss in the source and interstellar medium, but this has so far not been investigated.

The above results on abundances and energy spectra suggest that the rate of particle acceleration for a wide range of Z competes effectively with the rate of ionization loss at these low energies, which is not the case for a pure interstellar Fermi mechanism (Fermi 1954). The interesting possibility exists that the abundances in Figure 3 may be a reflection of cosmic ray origin in gaseous sources connected with regions where "alpha-particle-stable" nuclei are produced and where neutron build-up of elements has occurred.

IV. Acknowledgments

We are grateful to the staff of the Laboratory for Astrophysics and Space Research for the design, fabrication and testing of our experiment. We thank the Goddard Space Flight Center, NASA, for integrating the experiment into the OGO satellite and for the launch facilities and data reduction.

This research was supported in part by NASA Contract NAS-5-2133 and NASA Grant No. NsG 179-61, and by the U. S. Air Force Office of Scientific Research Grant AF-AFOSR-521-65.

References

‡ The OGO-I satellite was launched 4 September 1964 into an orbit with apogee 155,000 km. and an initial direction of 153° between the Sun-Earth line and the line of apsides. The orbit is inclined ~30° with respect to the equatorial plane.

Badhwar, G. D., Daniel, R. R. and Vijayalakshmi, B., 1962, Prog. Theoret. Phys. 28, 607-623.

Fan, C. Y., Gloeckler, G., and Simpson, J. A., 1965, J. Geophys. Res. 70, 3515-3527.

Fermi, E., 1954, Astrophys. J. 119, 1-6.

Fichtel, C. E., Guss, D. E., and Neelakantan, K. A., 1965, Phys. Rev. 138, B732-739.

Peters, B., Proceedings of the International Conference on Cosmic Rays and the Earth Storm, 1962, J. Phys. Soc. Japan 17, Suppl. A-III, 73-75.

Waddington, C. J., 1962, J. Phys. Soc. Japan 17, Suppl. A-III, 63-68: and references therein.

Figure Captions

Figure 1 (a) Cross section of detector elements for telescope with a geometrical factor 2.9 cm^2-Sr. D_1 and D_2 are Au-Si surface barrier detectors. Charged particles which pass through D_1 and D_2 and D_3 (Event a) are analyzed and contribute to the data in Figure 1.

The energy-loss determined by the pulse height in D_1 and the total energy derived from the pulse height in D_3 are shown for approximately 150 hours of raw data. The number of events falling in a given D_1 - D_3 channel is shown as a data point. The solid lines are calculated for selected elements and show the range end-points for penetration to detector D_4.

Figure 2 The number of stripped nuclei vs the deviation of D_1 pulse height channel number from the center ("0" channel number) of a solid curve over selected D_3 channel intervals.

From the center of the Carbon curve:

I - D_3 channels 8 - 25 (60 to 140 Mev/nucleon)

II - D_3 channels 26-36 (140 to 200 Mev/nucleon)

From the center of the Oxygen curve:

III - D_3 channels 8 - 32 (55 to 140 Mev/nucleon)

IV - D_3 channels 33 - 57 (140 to 240 Mev/nucleon)

Figure 3 Preliminary analysis of chemical abundances of the elements normalized to 0 = 100. The absolute flux for 0 is $5.4 \times 10^{-3}/M^2$ - Sr-Sec-Mev/nucleon in the kinetic energy range 30 Mev/nucleon to 240 Mev/nucleon.

Figure 4 Differential energy spectra based on approximately 150 hours of data.

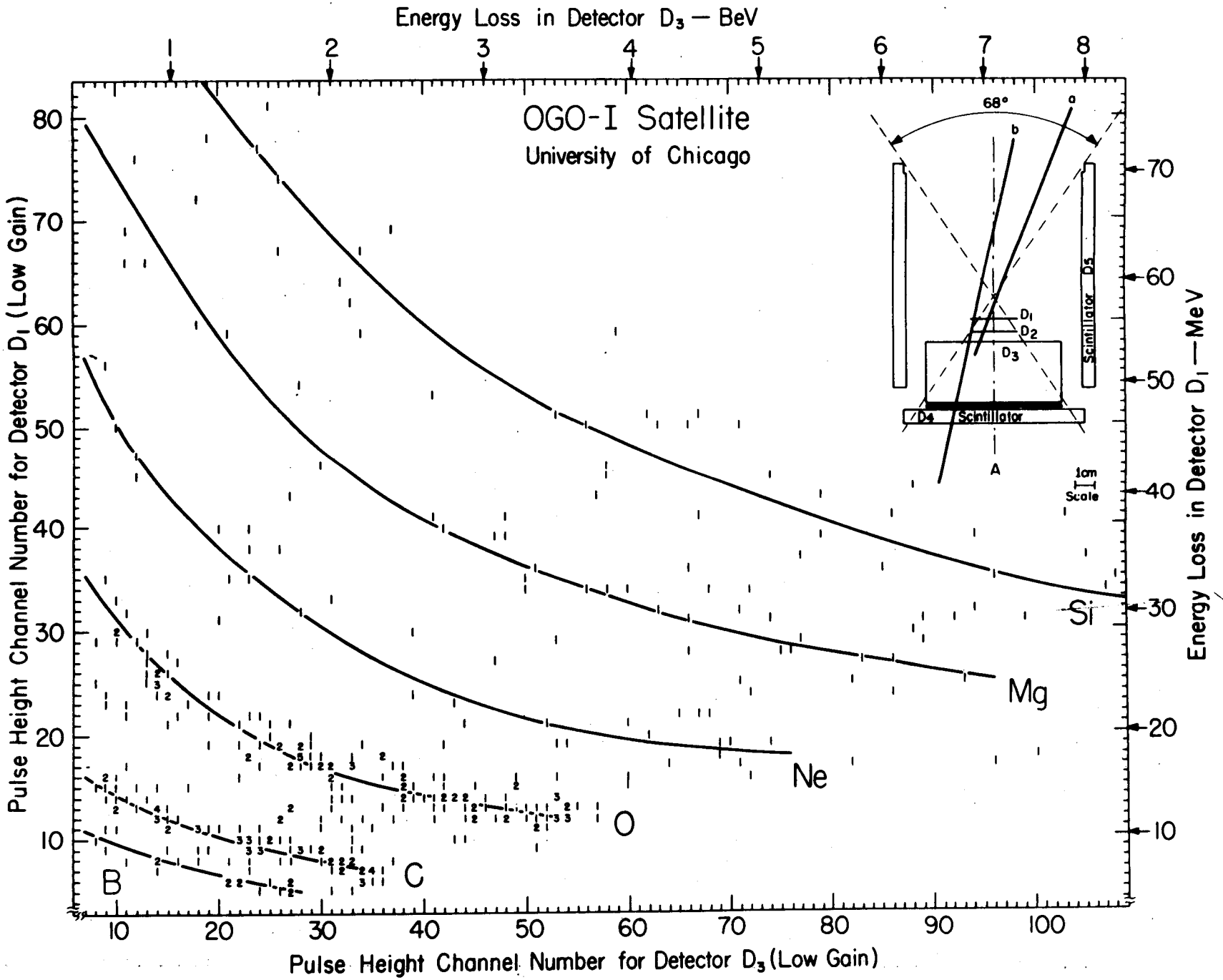
Energy Loss in Detector D_3 — BeV
OGO-I Satellite
University of Chicago
68°
a
b
D_1
D_2
D_3
Scintillator D_5
D_4 Scintillator
A
1g Scale
Si
Mg
Ne
O
C
B
Pulse Height Channel Number for Detector D_1 (Low Gain)
Energy Loss in Detector D_1 — MeV
Pulse Height Channel Number for Detector D_3 (Low Gain)

Fig. 1

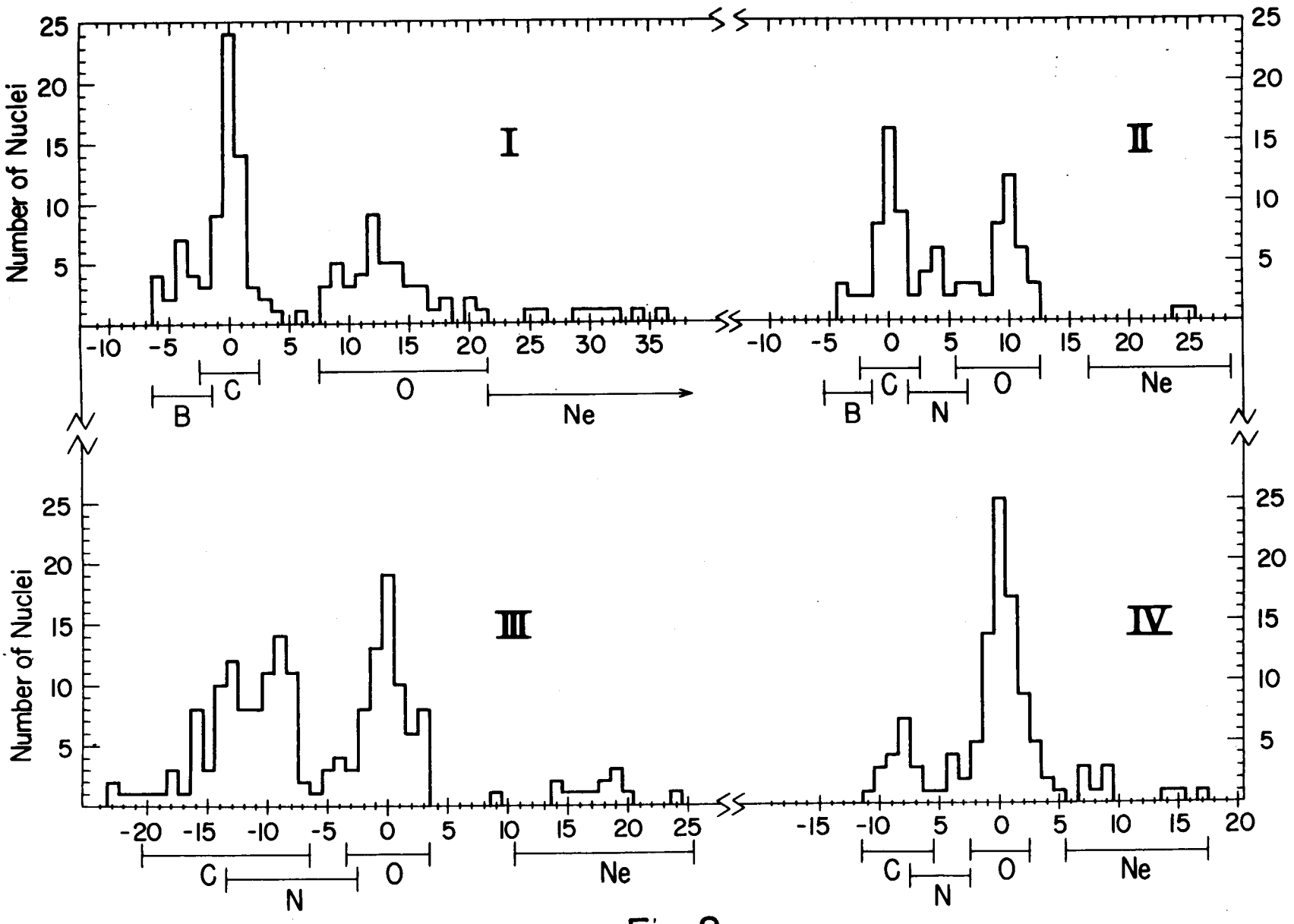

Fig. 2

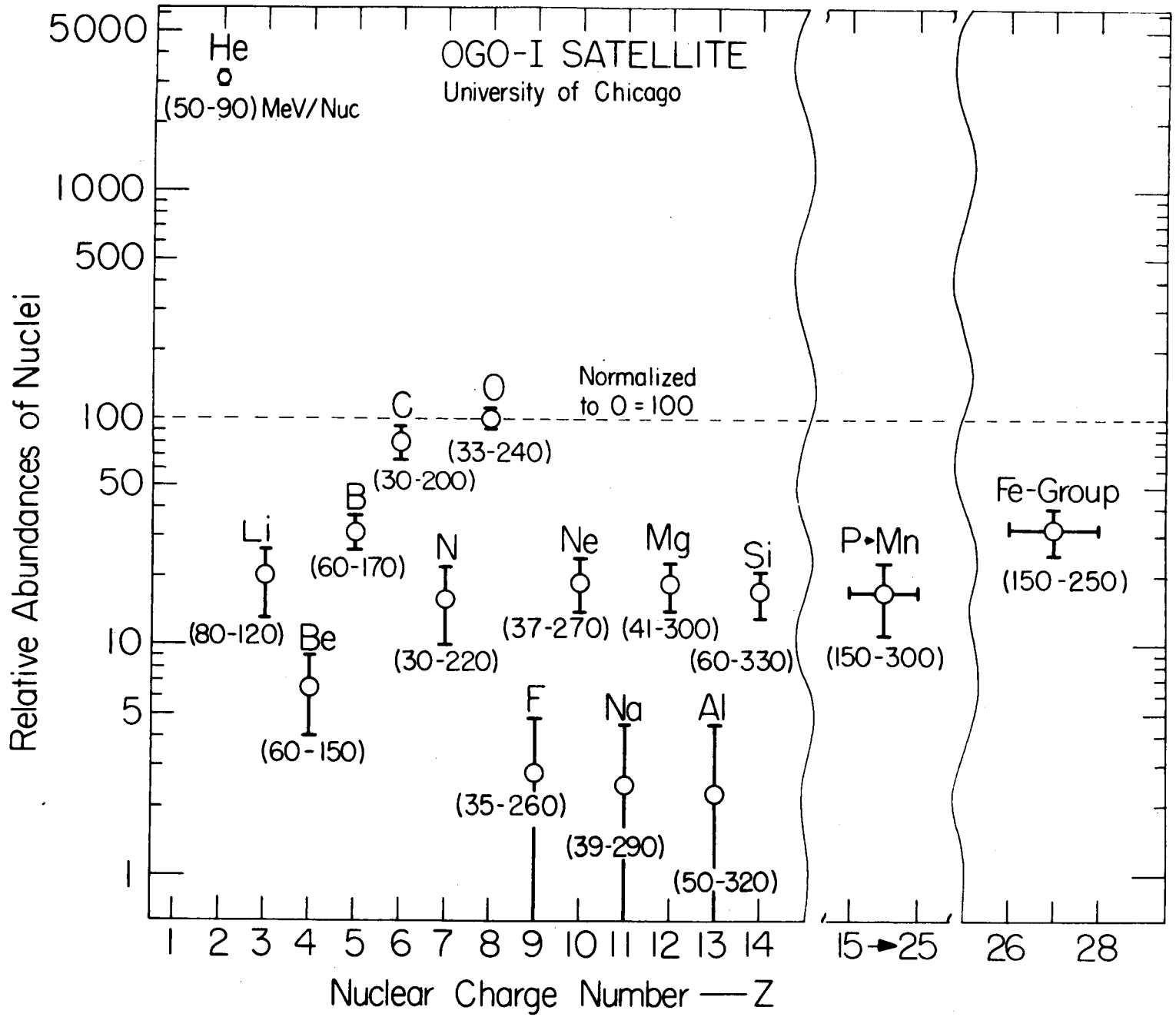
OGO-I SATELLITE
University of Chicago
He
(50-90) MeV/Nuc
Normalized
to O = 100
C
O
(30-200)
(33-240)
B
(60-170)
Li
(80-120)
Be
(60-150)
N
(30-220)
Ne
(37-270)
Mg
(41-300)
Si
(60-330)
P→Mn
(150-300)
Fe-Group
(150-250)
F
(35-260)
Na
(39-290)
Al
(50-320)
5000
1000
500
100
50
10
5
1
Relative Abundances of Nuclei
1 2 3 4 5 6 7 8 9 10 11 12 13 14
15→25
26 28
Nuclear Charge Number — Z

Fig. 3

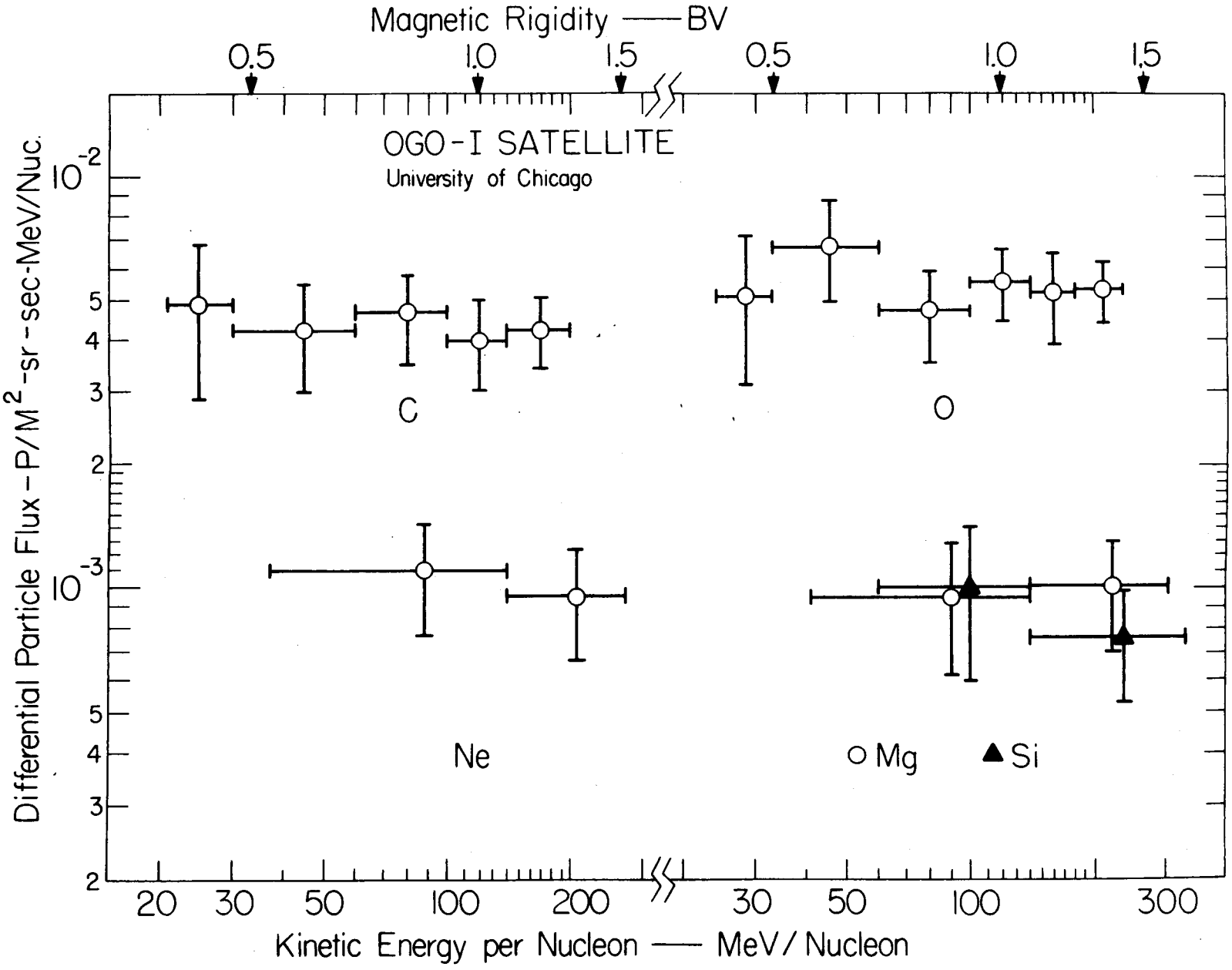
Magnetic Rigidity — BV
0.5
1.0
1.5
0.5
1.0
1.5
OGO-I SATELLITE
University of Chicago
Differential Particle Flux - P/M^2-sr-sec-MeV/Nuc
10^{-2}
5
4
3
2
10^{-3}
5
4
3
2
C
O
Ne
Mg
Si
20
30
50
100
200
30
50
100
300
Kinetic Energy per Nucleon — MeV/Nucleon

Fig. 4